

# Structure of the $\alpha$ and $\beta$ Polymorphs of Isotactic 1,4-*cis*-Poly(2-methyl-1,3-pentadiene)

D. R. Ferro,<sup>†</sup> S. Brückner,<sup>\*‡</sup> S. V. Meille,<sup>§</sup> and M. Ragazzi<sup>†</sup>

*Istituto di Chimica delle Macromolecole, CNR, Milano, Italy, Istituto di Idraulica, Università della Basilicata, I-85100 Potenza, Italy, and Dipartimento di Chimica, Politecnico di Milano, Milano, Italy*

Received February 13, 1990; Revised Manuscript Received July 26, 1990

**ABSTRACT:** The structures of two polymorphs of isotactic 1,4-*cis*-poly(2-methyl-1,3-pentadiene) are investigated through a computational procedure that simultaneously minimizes the conformational and the packing energy of a microcrystal of suitable dimensions. The results are compared with diffractometric data, and in both cases reliable structures are obtained by properly combining the indications coming from crystallographic analysis and energy calculations.

## 1. Introduction

Recently a computational approach to the evaluation of the potential energy in crystalline polymers was developed where both intra- and intermolecular interactions are simultaneously taken into account within each cycle of the optimization process.<sup>1</sup> This procedure can be applied provided that the crystalline lattice parameters and the space group symmetry of the structure to be investigated are specified. If they are unknown, a much more complex procedure is required where the possible molecular packings are to be investigated and lattice parameters are to be optimized.

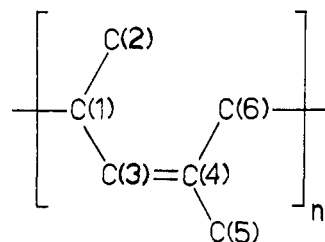
Comparison with experimental data, principally X-ray scattered intensities, is mandatory for assessing the reliability of the above-mentioned calculations, and this was done in two previous papers<sup>1,2</sup> where the crystal structures of two polymers, isotactic *trans*-1,4-poly(penta-1,3-diene) and poly(pivalolactone), determined from X-ray and electron diffraction data, were compared with the calculated models.

In both cases a good agreement was found, and it is worthwhile pointing out that both studies revealed that the observed models lay within rather broad minima of the energy hypersurface, so that less accurate computational procedures could easily lead to inaccurate structural models. The ultimate conclusion in the second paper<sup>2</sup> outlined the possibility of applying this procedure to unknown polymer crystal structures for obtaining reliable models to be subsequently tested and, eventually, refined with respect to the diffraction data.

An accurate energy evaluation can be very helpful both in the initial stages of a structural determination and, in case of low-quality experimental data, as an additional source of information leading to well-defined and more reliable structural models.

In the present work both aspects are investigated by studying the  $\alpha$ - and  $\beta$ -crystalline forms of isotactic 1,4-*cis*-poly(2-methyl-1,3-pentadiene) ( $\alpha$ - and  $\beta$ -iPMPD), shown with the atom numbering.

The structure of  $\alpha$ -iPMPD was already determined from powder X-ray diffraction data.<sup>3</sup> Low crystallinity and broadness of the diffraction peaks due to the presence of small and, possibly, strained crystallites together with the copresence of the  $\beta$  form, however, suggested some caution about accepting a too detailed description of the structure.



i-PMPD

Indeed, a somewhat short methyl-methyl interchain contact could be taken as an indication of slightly inaccurate packing.

Diffraction data for  $\beta$ -iPMPD are still poorer than those relative to  $\alpha$ -iPMPD. More specifically pure but unoriented  $\beta$ -phase samples can be obtained; however, because of extensive peak overlapping, only four broad maxima are observed in the powder diffraction profile of  $\beta$ -iPMPD, which is therefore inadequate for a full structural refinement. Lattice parameters and space group symmetry were tentatively derived from oriented-fiber patterns, which, due to the copresence of relevant amounts of  $\alpha$ -iPMPD, cannot be used to perform a full structural analysis.<sup>4</sup>

In the present paper we propose refined theoretical models assumed to be more reliable for both structures. In the case of  $\alpha$ -iPMPD the model obtained through energy minimization shows only a small worsening relative to the agreement with crystallographic data while attaining to a better geometry and much better packing contacts. In the case of  $\beta$ -iPMPD the observed profile is only used as a comparative test for different computed models, the best agreement being found in correspondence with the minimum energy structure.

## 2. Experimental Section

The procedures followed to fractionate the polymer as prepared and to obtain almost pure  $\beta$ -iPMPD are fully described in ref 4. The powder X-ray diffractions from the best crystallized  $\alpha$ -iPMPD and  $\beta$ -iPMPD, recorded on a Siemens D-500 diffractometer, are already reported in refs 3 and 4 (Figure 2), respectively, and are here simply repropounded as a comparison test for the different structural models.

## 3. Results and Discussion

Cell dimensions and space groups for the two phases are already reported in refs 3 and 4, but we list them in

<sup>†</sup> CNR.

<sup>‡</sup> Università della Basilicata.

<sup>§</sup> Politecnico di Milano.

Table I  
Crystal Data for  $\alpha$ -iPMPD and  $\beta$ -iPMPD

$\alpha$ -iPMPD	
$a = 10.74 \text{ \AA}$	orthorhombic
$b = 13.04 \text{ \AA}$	space group $Pbca$
$c = 7.87 \text{ \AA}$	$Z = 4, D_c = 1.00 \text{ g cm}^{-3}$
$\beta$ -iPMPD	
$a = 9.30 \text{ \AA}$	orthorhombic
$b = 7.73 \text{ \AA}$	space group $P2_12_12_1$
$c = 7.90 \text{ \AA}$	$Z = 4, D_c = 0.96 \text{ g cm}^{-3}$

Table II  
Internal Coordinates for iPMPD, Isolated Chain  
( $h = 3.95 \text{ \AA}$ )

Bond Lengths ( $\text{\AA}$ )			
C(1)–C(2)	1.538	C(4)–C(5)	1.511
C(1)–C(3)	1.514	C(4)–C(6)	1.513
C(3)–C(4)	1.345	C(6)–C(1)	1.541
Bond Angles (deg)			
C(6)–C(1)–C(3)	110.4	C(1)–C(3)–C(4)	129.0
C(2)–C(1)–C(3)	109.0	C(3)–C(4)–C(6)	125.9
C(6)–C(1)–C(2)	111.1	C(3)–C(4)–C(5)	117.9
C(5)–C(4)–C(6)	116.2	C(1)–C(6)–C(4)	112.9
Torsion Angles (deg)			
C(1)–C(3)–C(4)–C(6)	1.0	C(4)–C(6)–C(1)–C(3)	178.8
C(3)–C(4)–C(6)–C(1)	112.9	C(6)–C(1)–C(3)–C(4)	–110.6

Table I for sake of expediency. The  $\alpha$ -iPMPD structure requires polymer chains located on a 2-fold screw axis, so that a  $2_1$  symmetry is imposed to the macromolecule with a repeat period of  $7.87 \text{ \AA}$  ( $3.935 \text{ \AA}$ /monomer unit). The same periodicity ( $3.95 \text{ \AA}$ ) is observed in  $\beta$ -iPMPD, and this fact, together with density requirements, suggests that also in this case the macromolecule is to be located on the binary screw axis parallel to  $c$  in the  $P2_12_12_1$  space group. This constraint is very useful in limiting the number of structural parameters to be varied in the search of the minimum energy structure.

(a) **Isolated Chain.** The conformational energy of the isolated chain was first minimized by imposing the  $2_1$  helical symmetry. For simplicity the atomic coordinates obtained by Brückner et al.<sup>3</sup> for  $\alpha$ -iPMPD were chosen as the starting point. As in the previous papers,<sup>1,2</sup> the force-field parameters were taken from Allinger,<sup>5</sup> and the energy minimization was performed in Cartesian coordinates with no geometrical constraint except for those explicitly noted (i.e., 2-fold helical symmetry in this case).

The energy minimum was found to correspond to an axial advancement ( $h$ ) of  $3.90 \text{ \AA}$ . The closeness of this value with those observed in  $\alpha$ -iPMPD and  $\beta$ -iPMPD is a first indication that the force field used in the present calculations is well suited for studying this polymer. By imposing  $h = 3.95 \text{ \AA}$ , we find a model with energy only  $0.04 \text{ kcal/mol}$  higher than the absolute minimum; this model was the starting point for the calculations on  $\beta$ -iPMPD, while a model with  $h = 3.935 \text{ \AA}$  was the starting point for the calculations on  $\alpha$ -iPMPD. In Table II we report the geometrical data relative to the isolated chain with  $h = 3.95 \text{ \AA}$ , while those relative to the chain with  $h = 3.935 \text{ \AA}$  are omitted in view of the small differences involved. A stereographic view of the isolated chain is shown in Figure 1.

(b)  **$\alpha$ -iPMPD.** As already stated, a structural model of  $\alpha$ -iPMPD (hereafter model I) was previously proposed on the basis of a best fit to the powder X-ray diffraction profile.<sup>3</sup>

Energy minimization, applied to the chain defined in the preceding section, led to a structure (model II) with a total energy of  $-2.70 \text{ kcal/mol}$ , referred to one monomer

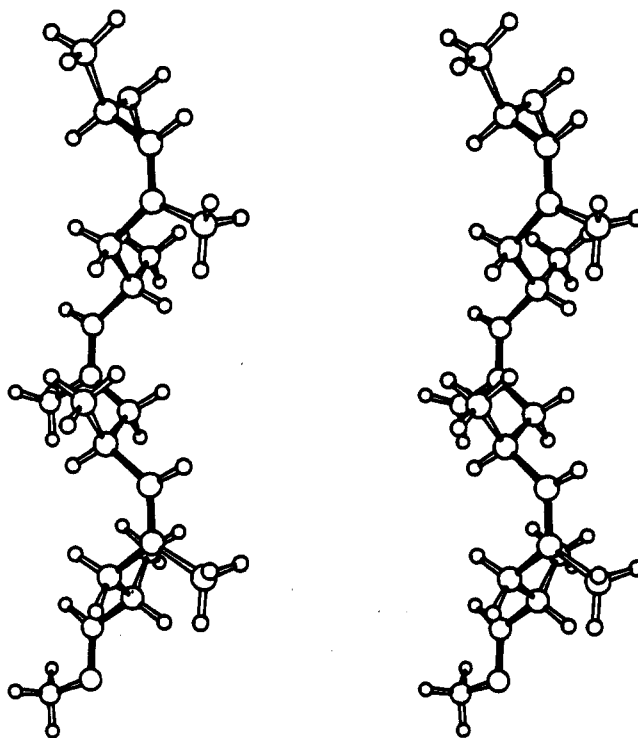


Figure 1. Stereographic view of the isolated chain of i-PMPD.

Table III  
Fractional and Internal Coordinates for Model II of  $\alpha$ -iPMPD

atom	$x$	$y$	$z$
C(1)	0.2879	–0.0453	0.0409
C(2)	0.3461	–0.1243	0.1624
C(3)	0.1963	–0.0989	–0.0747
C(4)	0.1918	–0.0993	–0.2453
C(5)	0.0915	–0.1622	–0.3300
C(6)	0.2788	–0.0411	–0.3614
Bond Lengths ( $\text{\AA}$ )			
C(1)–C(2)	1.539	C(4)–C(5)	1.509
C(1)–C(3)	1.512	C(4)–C(6)	1.511
C(3)–C(4)	1.344	C(6)–C(1)	1.540
Bond Angles (deg)			
C(6)–C(1)–C(3)	109.7	C(1)–C(3)–C(4)	128.8
C(2)–C(1)–C(3)	109.1	C(3)–C(4)–C(6)	125.5
C(6)–C(1)–C(2)	111.7	C(3)–C(4)–C(5)	118.0
C(5)–C(4)–C(6)	116.5	C(1)–C(6)–C(4)	112.4
Torsion Angles (deg)			
C(1)–C(3)–C(4)–C(6)	2.0	C(4)–C(6)–C(1)–C(3)	179.0
C(3)–C(4)–C(6)–C(1)	112.1	C(6)–C(1)–C(3)–C(4)	–111.9

unit, and showing a rms deviation of  $0.47 \text{ \AA}$  relative to the carbon atom positions of model I. The considerable deviation from the original coordinates is mainly due to a negative shift of the chain along the  $c$  axis ( $-0.45 \text{ \AA}$ ) and, to a lesser extent, to some rearrangement of the internal geometry, which is quite close to that computed for the isolated chain. In Table III we report the fractional and internal coordinates for model II while, for sake of comparison, the same data for model I (see ref 3) are reported in Table IV.

(c)  **$\beta$ -iPMPD.** The microcrystal of  $\beta$ -iPMPD was generated according to the  $P2_12_12_1$  space group, by using the cell parameters obtained from X-ray diffraction patterns,<sup>4</sup> and listed in Table I. As already stated there are strong indications for locating the macromolecule on the binary screw axis parallel to  $c$ . For an exhaustive analysis of the  $\beta$  form, the iPMPD helix, corresponding to the lowest conformational energy in the isolated state,

**Table IV**  
Fractional and Internal Coordinates for Model I of  $\alpha$ -iPMPD (See Reference 3)

atom	x	y	z
C(1)	0.2800	-0.0492	-0.0190
C(2)	0.3444	-0.1214	0.1066
C(3)	0.1901	-0.0982	-0.1403
C(4)	0.1912	-0.0876	-0.3084
C(5)	0.1005	-0.1650	-0.3763
C(6)	0.2858	-0.0369	-0.4207

## Bond Lengths (Å)

C(1)-C(2)	1.535	C(4)-C(5)	1.50
C(1)-C(3)	1.50	C(4)-C(6)	1.50
C(3)-C(4)	1.33	C(6)-C(1)	1.535

## Bond Angles (deg)

C(6)-C(1)-C(3)	110	C(1)-C(3)-C(4)	126
C(2)-C(1)-C(3)	116	C(3)-C(4)-C(6)	129
C(6)-C(1)-C(2)	109	C(3)-C(4)-C(5)	106
C(5)-C(4)-C(6)	122	C(1)-C(6)-C(4)	108

## Torsion Angles (deg)

C(1)-C(3)-C(4)-C(6)	-8	C(4)-C(6)-C(1)-C(3)	177
C(3)-C(4)-C(6)-C(1)	121	C(6)-C(1)-C(3)-C(4)	-108

## iPMPD

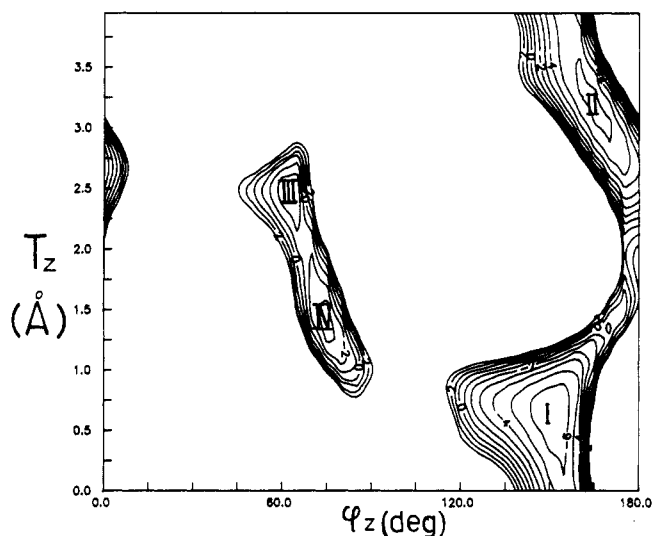


**Figure 2.** Energy map obtained in the case of  $\beta$ -iPMPD. The monomer unit is treated as a rigid body, and  $\phi_z$  and  $T_z$  are, respectively, the rotation and the translation of the helix relative to its axis.

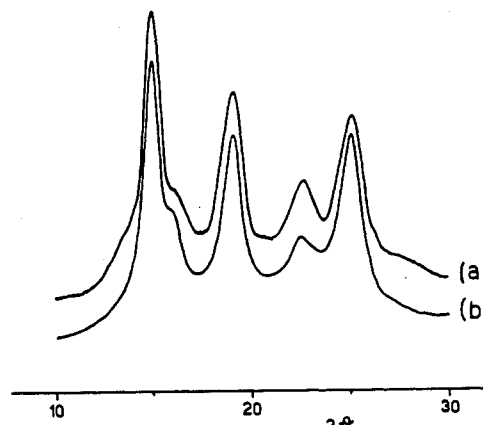
was treated as a rigid body for calculating the intermolecular energy as a function of the 2 degrees of freedom allowed, i.e., a rotation around the helix axis ( $\phi_z$ ) and a translation along the same axis ( $T_z$ ). The assumption of the isolated chain geometry appeared reasonable for a first analysis of the low-energy structures, since for the  $\alpha$  form the chain conformation is close to that found for the isolated chain.

The systematic variations of the two variables  $\phi_z$  and  $T_z$  gave rise to a bidimensional energy map, which is shown in Figure 2. The four minima visible in the map were subjected to full energy minimization, removing the rigid-body constraint. This calculation led to the four structures reported in Table V. Minima I and II differ by only 0.23 kcal/mol and were further investigated with reference to the observed powder X-ray diffraction profile from pure  $\beta$ -iPMPD. This profile is not suitable for a structural refinement, being characterized by only four broad peaks in the low  $2\theta$  region. We therefore adopted it as a comparison test for models I and II, the best fit being only performed through the adjustment of nonstructural pa-

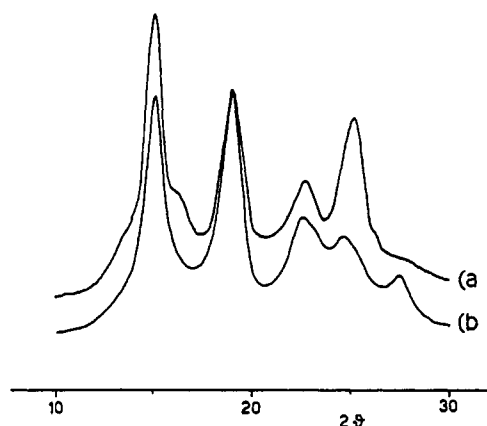
**Table V**  
Four Minima of  $\beta$ -iPMPD (See Figure 2)<sup>a</sup>

	$\phi_z$ , deg	$T_z$ , Å	$E_{\text{total}}$ , kcal/mol
I	151.9	0.65	-2.44
II	168.2	3.17	-2.21
III	82.1	2.28	-0.63
IV	82.8	1.32	-0.49

<sup>a</sup> Numerical values of  $\phi_z$  and  $T_z$  are arbitrarily represented by the cylindrical coordinates of atom C(6).



## model I



## model II

**Figure 3.**  $\beta$ -iPMPD. (a) The observed profile (curve a) is compared with the profile calculated with model I (curve b). (b) The same comparison is drawn for model II.

rameters, i.e., a segmented base line and peak half-height widths. Results show a marked preference for model I, the lowest energy one, as may be seen in Figure 3 where the observed profile (curve a) is compared with the calculated profiles obtained with model I and model II (curves b). We then propose model I for the crystal structure of  $\beta$ -iPMPD and report the corresponding atomic coordinates in Table VI.

**(d)  $\alpha$ -iPMPD and  $\beta$ -iPMPD Mixed Polymorphs.** The atomic coordinates of model II of  $\alpha$ -iPMPD were used to compute, through a procedure already described,<sup>6</sup> a powder diffraction profile to be compared with the observed one. The disagreement factor is  $R_2 = 0.37$  while for model I it was 0.28.<sup>3</sup> The difference is relevant, but the presence of significant  $\beta$ -iPMPD contributions to the observed profile may somehow reduce the significance of this disagreement factor, since they introduce some uncertainty about the values of the "pure"  $\alpha$ -iPMPD profile. To prove this statement, we have computed the powder X-ray diffraction profile of  $\alpha$ -iPMPD, taking into account also the contribution of  $\beta$ -iPMPD, whose structure

Table VI  
Fractional and Internal Coordinates for Model I of  $\beta$ -iPMPD

atom	<i>x</i>	<i>y</i>	<i>z</i>
C(1)	0.3170	-0.0426	0.1788
C(2)	0.4273	-0.1204	0.0552
C(3)	0.2654	-0.1836	0.2971
C(4)	0.2637	-0.1853	0.4673
C(5)	0.2097	-0.3464	0.5550
C(6)	0.1899	0.0387	0.0820

Bond Lengths (Å)			
C(1)-C(2)	1.538	C(4)-C(5)	1.510
C(1)-C(3)	1.514	C(4)-C(6)	1.514
C(3)-C(4)	1.345	C(6)-C(1)	1.542

Bond Angles (deg)			
C(6)-C(1)-C(3)	110.9	C(1)-C(3)-C(4)	128.8
C(2)-C(1)-C(3)	108.7	C(3)-C(4)-C(6)	125.5
C(6)-C(1)-C(2)	111.7	C(3)-C(4)-C(5)	118.0
C(5)-C(4)-C(6)	116.5	C(1)-C(6)-C(4)	112.4

Torsion Angles (deg)			
C(1)-C(3)-C(4)-C(6)	2.0	C(4)-C(6)-C(1)-C(3)	179.0
C(3)-C(4)-C(6)-C(1)	112.1	C(6)-C(1)-C(3)-C(4)	-111.9

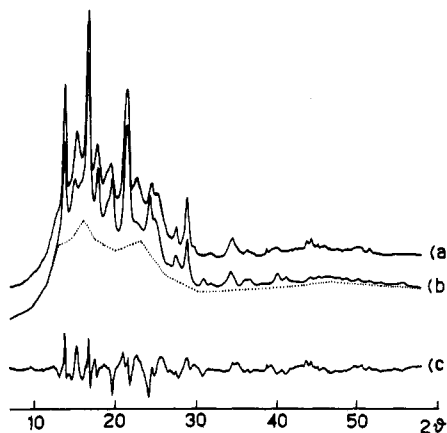
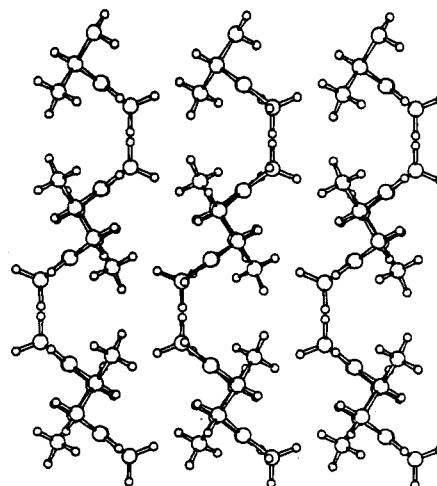


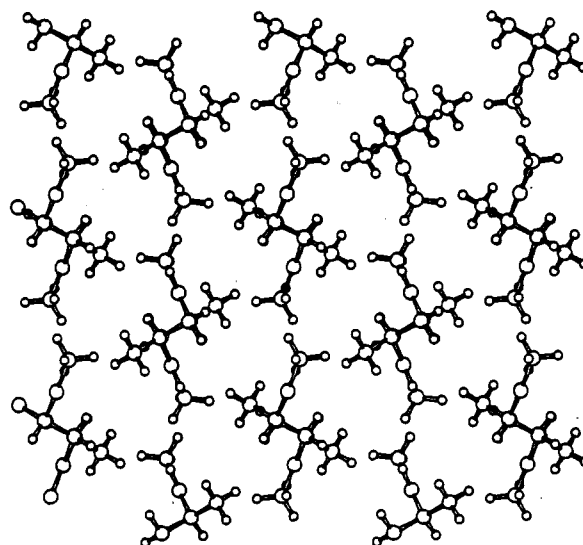
Figure 4. Observed (curve a) profile compared with the profile calculated with model II of  $\alpha$ -iPMPD and with the contribution of model I of  $\beta$ -iPMPD (curve b). Curve c is the difference profile, and the dashed line represents the background contribution.

is now determined (see model I of  $\beta$ -iPMPD). The resulting calculated profile is therefore the superposition of the two diffraction diagrams pertaining separately to  $\alpha$ - and  $\beta$ -iPMPD. The best fit procedure was carried out by optimizing the base-line parameters and a scale factor that represents the amount of  $\beta$ -iPMPD present. The disagreement factors computed for models I and II of  $\alpha$ -iPMPD in the presence of  $\beta$ -iPMPD were 0.20 and 0.22, respectively, with a substantial reduction of the difference between them and, therefore, an increase of the importance of model II as a reliable representation of the structure of  $\alpha$ -iPMPD. The slight worsening in the disagreement factor is in fact largely compensated by a less strained internal geometry and better packing contacts. For example, the methyl-methyl intermolecular contact of 3.34 Å present in model I is alleviated to 3.75 Å in model II, all other contacts being within acceptable ranges.

It is clear now that model I was rather heavily biased by the presence of the unknown, at that time,  $\beta$  structure in the observed profile, and we consider model II to represent a substantial improvement in the description of the structure of  $\alpha$ -iPMPD. A more precise definition of the position occupied by the chain along its helix axis ( $T_z$  translation) within the limits represented by models I and II is difficult due to the low sensitivity of the crystallographic disagreement factor and of the potential energy



(a)



(b)

Figure 5. Microcrystal of  $\alpha$ -iPMPD, considered in the final refinement of the most stable structure, viewed along *c*. (b) The microcrystal of  $\beta$ -iPMPD viewed along *c*. Molecular models drawn with the program SCHAKAL.<sup>7</sup>

function toward such a variable. In Figure 4 we show a comparison between the observed (curve a) profile and the profile calculated with model II and the additional contribution of  $\beta$ -iPMPD (curve b); curve c is the difference profile, and the dashed line is the background contribution. In Figure 5a we show the microcrystal of  $\alpha$ -iPMPD, considered in the final refinement, viewed along *c*, while in Figure 5b the same view is applied to the microcrystal of  $\beta$ -iPMPD; the molecular models were drawn with the program SCHAKAL.<sup>7</sup>

#### 4. Concluding Remarks

The minimum energy structure of  $\alpha$ -iPMPD (model II) is 0.26 kcal/mol lower than that of model I of  $\beta$ -iPMPD. A small difference that justifies the observed polymorphism of iPMPD and is also in qualitative agreement with the higher melting point observed for  $\alpha$ -iPMPD (175 °C) relative to that of  $\beta$ -iPMPD (165 °C).

We also point out that in this case, unlike the case of poly(pivalolactone),<sup>2</sup> the two polymorphs show an almost undistinguishable geometry of the polymer chain.

Accurate conformational and packing energy calculations prove again to be a valuable support to structure determination, in particular when observed crystallographic data are of poor quality, a rather common event in polymer crystallography. The results of the present analysis, together with those previously reported for other polymer structures,<sup>1,2</sup> reveal the usefulness of developing an integrated computational procedure where the crystallographic and the energetic approaches are merged together.

## References and Notes

- (1) Ferro D. R.; Brückner, S. *Macromolecules* **1989**, *22*, 2359.
- (2) Ferro, D. R.; Brückner, S.; Meille, S. V.; Ragazzi, M. *Macromolecules* **1990**, *23*, 1676.
- (3) Brückner, S.; Meille, S. V.; Porzio, W.; Ricci, G. *Makromol. Chem.* **1988**, *189*, 2145.
- (4) Cabassi, F.; Porzio, W.; Ricci, G.; Brückner, S.; Meille, S. V.; Porri, L. *Makromol. Chem.* **1988**, *189*, 2135.
- (5) Allinger, N. L.; Yuh, Y. H. *QCPE* **1980**, *12*, 395.
- (6) Immirzi, A. *Acta Crystallogr.* **1980**, *B36*, 2378.
- (7) Keller, G. E. *Chem. Unserer Zeit* **1980**, *14*, 56.

**Registry No.** iPMPD, 34540-02-8.